Molecular Diversity (2024) 28:97–110
https://doi.org/10.1007/s11030-023-10616-8

ORIGINAL ARTICLE

Synthesis and studies of new purines/pyrimidine derivatives as multi-targeted agents involving various receptor sites in the immune system

Gurmeet Kaur[1] · Manisha Bansal[3] · Hafiz Muzzammel Rehman[2] · Mandeep Kaur[1] · Amandeep Kaur[1]

Received: 1 June 2022 / Accepted: 23 January 2023 / Published online: 28 February 2023

Abstract

Pro-inflammation, which is developed due to the increased production of cytokines, mainly interleukin-6 (IL-6), during the working of immune system pathways, becomes a major concern these days for many researchers. So, it is desired to design, screen, and synthesize new molecules with multi-parametric features showing their efficacy for Toll-like receptors (TLRs) and inhibiting the disease-causing receptor sites like viral infections, cancers, etc. along with controlling inflammation, fever, and other side effects during such pathways. Further, looking at the literature, curcumin a multi-targeted agent is showing its efficiency toward various receptor sites involved in many diseases as mentioned above. This fascinated us to build up new molecules which behave like curcumin with minimum side effects. In silico studies, involving ADMET studies, toxicological data, and docking analyses, of newly synthesized compounds (3–5) along with tautomers of curcumin i.e., (1–2), and some reported compounds like 9 and 10 have been studied in detail. Great emphasis has been made on analyzing binding energies, protein–ligand structural interactions, stabilization of newly synthesized molecules against various selected receptor sites using such computational tools. Compound 3 is the most efficient multifunctional agent, which has shown its potential toward most of the receptor sites in docking analysis. It has also responded well in Molecular dynamics (MD) simulation toward 5ZLN, 4RJ3, 4YO9, 4YOJ, and 1I1R sites. Finally, studies were extended to understand in vitro anti-inflammatory activity for particularly compound 3 in comparison to diclofenac and curcumin, which signifies the efficiency of compound 3.

Graphical abstract

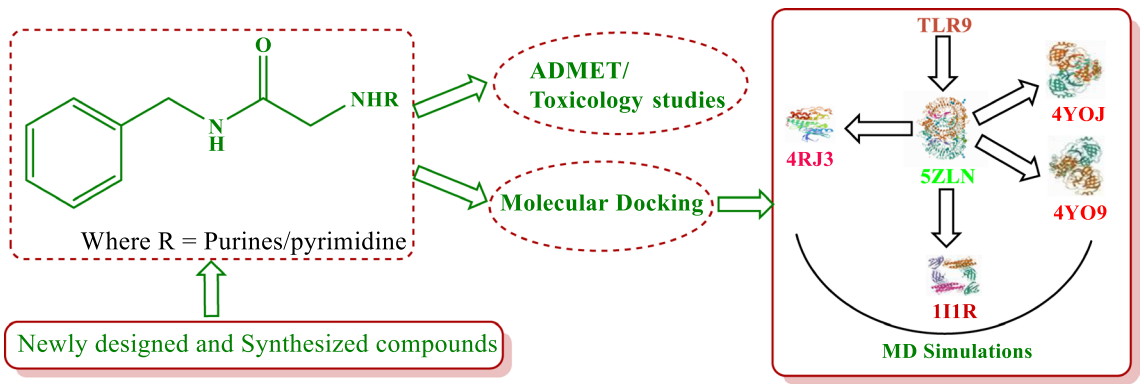

Keywords Curcumin · TLR9 · Docking analysis · MD simulations · Anti-inflammatory activity in vitro

✉ Manisha Bansal
jindal_manisha@yahoo.co.in

Extended author information available on the last page of the article

Introduction

Infectious challenges using various receptor families that can identify pathogen-expressed molecules like viral RNA or bacterial DNA have been detected by the human immune system [1]. During these pathways, the involvement of Toll-like receptors (TLRs) causes a release of cytokines which lead to pro-inflammatory action along with the prevention of different diseases [2–4]. These abnormal actions lead to fever and in some cases, acute diseases which are becoming a serious point of discussion for various research groups. *Such studies made us think that whether any ligand which is showing its efficacy toward various TLRs can be used to cure only infectious disease or it can also lead to reduce the inflammation, fever, headache* etc. *due to over expression of interleukin-6 (IL-6)* [5–15].

It fascinated us to initiate our work by taking curcumin as a multifaceted agent and used against various diseases such as anti-inflammatory, antiviral, anticancer, antioxidant, antimicrobial, etc. which made it a wonderful agent [16–24]. The structural framework of curcumin (1) consists of two aromatic rings with a dicarbonyl linker in the center as shown in Fig. 1. This attracted us to design new molecules with bioactive precursors like Purines/pyrimidine as aromatic moieties and containing linker moiety, but with hetero atom like nitrogen in the linker part. The presence of nitrogen is proposed to increase the solubility property

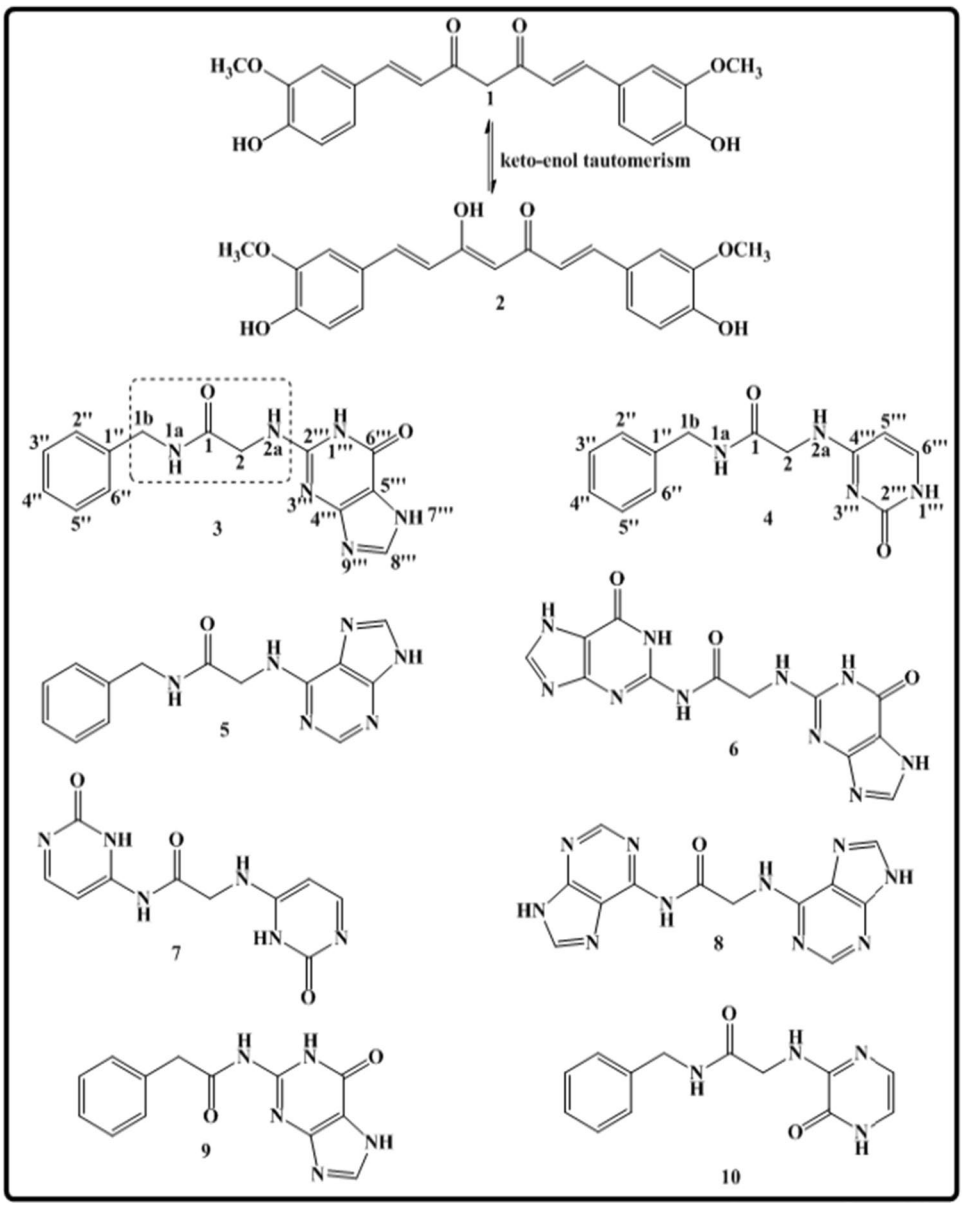

Fig. 1 Structures of curcumin (1–2), newly designed (3–8), and reported (9–10) compounds

leading to better bioavailability and hence may better fit in the pocket of various receptor sites.

Therefore, the present piece of work deals with the design, synthesis, and in silico analyses of Purines/pyrimidine derivatives, whose structural framework resembles curcumin, but with better moieties and improved properties. Detailed in silico studies involving ADMET studies, toxicology effects, docking analyses, and MD simulation were carried out to understand the responses of new compounds in comparison to curcumin as well as some reported compounds. Finally, in vitro anti-inflammatory activity will be carried out for the most efficient molecule, and a comparative analysis with curcumin and diclofenac will be taken.

Results and discussion

Computational studies

The physicochemical studies of newly designed molecules using ADMET tools

ADMET studies, using various computational tools, provide detailed data regarding the physicochemical parameters of the new set of molecules and also helps in screening and selecting the most suitable molecules for synthesis and further studies. Even though curcumin is known to be effective against numerous diseases and helps to improve the immune system, it does not cure them completely. Studies of structural features are important to design a new pharmacophore for the development of new molecules with minimum side effects. One of the major drawbacks of curcumin is its low bioavailability and poor solubility [25–29]. The presence of various substituents, their position, number, and pattern of linker affects the properties of the given molecule. In the case of curcumin, the presence of 1,3-dicarbonyl linker plays a vital role in the anticancer activity. To understand such features, a list of molecules was designed (3–8), and subjected to their ADMET studies. Their physicochemical properties were discussed and compared with reported compounds (9–10) along with both the tautomers of curcumin (1 and 2) (Fig. 1 and Table 1).

The solubility parameter of any compound can be enhanced, either by increasing the number of hydroxyl groups or by increasing the number of hetero atoms such as N, S, or O which in turn increases the polarity and hence affects the solubility of the molecule. As shown in Table 1, the hydrogen bond acceptor value (HBA) of curcumin **(1)** and its enolic form **(2)** is more than that of hydrogen bond donor (HBD) values. On the other hand, both these values are in the range (approx 3–4) in most of the other compounds **(3–10)**. Another major observation is the values of topological surface area (TPSA) which is lesser than or equal to 140 $Å^2$ [30]. From (ST-1), it is observed that compound 3, 4, 5, 9, and10 which are following drug-likeness rules tends to justify the rule of five and do not enter the blood–brain

Table 1 Physicochemical properties of compounds (1–10) using SwissADME software

Compounds	MW[a]	TPSA[b]	HBA[c]	HBD[d]	LogP[e]	LogS[f]	DL[g]	GI[h]	BBB[i]	P-gp[j]
1	368.38	93.06	6	2	3.37	− 4.45	Yes	High	No	No
2	368.38	96.22	6	3	3.17	− 3.61	Yes	High	No	No
3	298.30	115.56	4	4	0.52	− 5.44	Yes	High	No	No
4	258.28	86.88	3	3	0.77	− 4.94	Yes	High	No	No
5	282.30	95.59	4	3	1.13	− 5.54	Yes	High	No	Yes
6	342.27	189.99	7	6	-1.32	− 4.69	No	Low	No	No
7	262.22	132.63	5	4	-0.99	− 3.70	No	Low	No	No
8	310.27	150.05	7	4	-0.20	− 4.89	No	Low	No	No
9	269.26	103.53	4	4	0.72	− 5.00	Yes	High	No	No
10	258.28	86.88	3	3	0.71	− 4.94	Yes	High	No	No

[a–j]Are physicochemical parameters calculated by SwissADME software

[a]Molecular weight

[b]Topological polar surface area

[c]Hydrogen bond acceptors;

[d]Hydrogen bond donors

[e]lipophilicity

[f]Water solubility parameter

[g]Drug likeness

[h]Gastrointestinal absorption

[i]Blood brain barrier

[j]P-glycoprotein substrate

barrier having the TPSA value above 70 $Å^2$ [31, 32]. From Table 1, these compounds are also showing high GI absorption. P-glycoprotein and permeability glycoprotein substrate are involved in the efflux mechanism which is ATP dependent and is responsible for decreased drug accumulation in multidrug resistance cells and often mediates the development of resistance to anticancer drugs [33].

Toxicological studies

The toxicological behavior of these molecules was predicted using OSIRIS Data Warrior software (http://www.openmolecules.org/datawarrior/) (ST-1) [34]. Compounds **(1–2, 4–5, and 9–10)** were non-toxic toward mutagenic, tumorigenic, reproductive systems and irritants except compound 3, which has shown minor toxicity toward mutagenic system. So, from these results, compounds **(3–5)** were selected for further synthesis and docking analysis.

Target prediction analyses

Before undergoing docking analysis, the reference molecules 1 and 2 were subjected to Swiss Target Prediction analysis using SwissADME tools (SF-1, SF-2). As both the tautomers of curcumin (1–2) have shown highest binding probability toward TLRs, therefore, this has been taken primarily to analyze the further results. Present work deals with understanding the multi-parametric features of newly synthesized compounds against all the receptors sites, which are related to innate immune system pathways.

Molecular docking analysis

For docking analysis, Chimera 1.15 and Biovia (Discovery studio v21.1.0.20298) have been used. Three trials have been taken for the average vina score toward each receptor site (ST-2). Also, side chain A for all target sites was taken, and specifications of center of grid for all sites were optimized as shown in (ST-3). To understand the structural features of the reference compounds **(1–2)** and to compare the results with newly synthesized compounds **(3–5)** and reported compounds **(9–10)** [35, 36], almost all the target sites of TLR9 were taken from PDB files (PDB code:—3WPD, 3WPE, 3WPF, 3WPG, 3WPH, 3WPI, 3WPB, 3WPC, 4QDH, 5ZLN, 5Y3J, 5Y3L, 5Y3K, 5Y3M (ST-2)) and were screened using Autodock Vina.

Molecular docking studies of selected TLR9 sites with all ligands (1–5, 9–10)

Out of all the target sites mentioned above, compounds 1–2 have shown good binding energy for 5ZLN site (ST-2). All the newly synthesized compounds (3–5) and reported compounds (9–10) were subjected for docking studies toward 5ZLN site. Table 2 represents that compound 3 was the most efficient among all the other sets of molecules with average binding energy − 8.1 kcal/mol.

Table 2 Docking analysis toward various receptor sites

Compound	Binding energies (kcal/mol)				
	5ZLN	4RJ3	4YOJ	4YO9	1I1R
1	− 7.3	− 6.5	− 6.5	− 6.3	− 5.4
2	− 7.6	− 7.4	− 6.9	− 7.5	− 6.0
3	**− 8.1**	**− 7.8**	**− 7.5**	**− 7.6**	**− 7.3**
4	− 6.5	− 6.2	− 6.0	− 6.0	− 5.8
5	− 7.2	**− 8.0**	− 6.8	− 7.3	− 6.5
9	**− 7.8**	**− 7.8**	**− 7.1**	**− 7.4**	− 6.5
10	− 6.4	− 6.6	− 6.3	− 5.9	− 5.7

The significance of bold values is for the more efficient results

Figure 2 represents various binding interactions of the 5ZLN receptor site with various compounds (1–5, and 9). Compound 1 has not shown conventional hydrogen bond interaction (CHB) with linker, whereas the enolic form i.e., compound 2 was involved in CHB interaction with that of linker portion. On the other hand, CHB interactions of compound 3 have a minimum bond distance of 2.0217 Å with ASP A: 469 (ST-4). Moreover, it has also shown interaction with hydrogen of NH (at position **1'''** and **2a** in Fig. 1), whereas no such interactions were observed in the linker part of compounds 4, 5, and 9. Overall compound 3 seems to interact better than all other compounds not only with bond distance or hydrogen bond interaction but also in terms of minimum hydrophobic interactions. With the increased HBD (hence TPSA values) for compounds 1 < 2 = 3 (from ADMET studies as shown in Table 1), an increase in the hydrogen bond interactions in docking studies was also detected (Fig. 2). Another major finding was observed while comparing the structure of compound 3 with that of compound 9 (the structure of which resembles that of compound 3) [36]. Although, there was a lot of structural similarity between the two compounds and also HBD and TPSA of these were almost similar then also compound 9 showed lesser CHB interaction and increased hydrophobic interactions which made compound 9 less potent than compound 3. *This signified that not only the presence of hetero atoms mainly nitrogen, in the linker part but also the position of the hetero atom played a vital role in structural interactions.*

Molecular docking studies of breast cancer (PDB ID: 4RJ3) with various ligands (1–5, 9–12)

A specific piece of research was seen, in which TLR9 was somewhere indirectly related to breast cancer studies [6]. Preclinical studies for immunotherapeutic approach

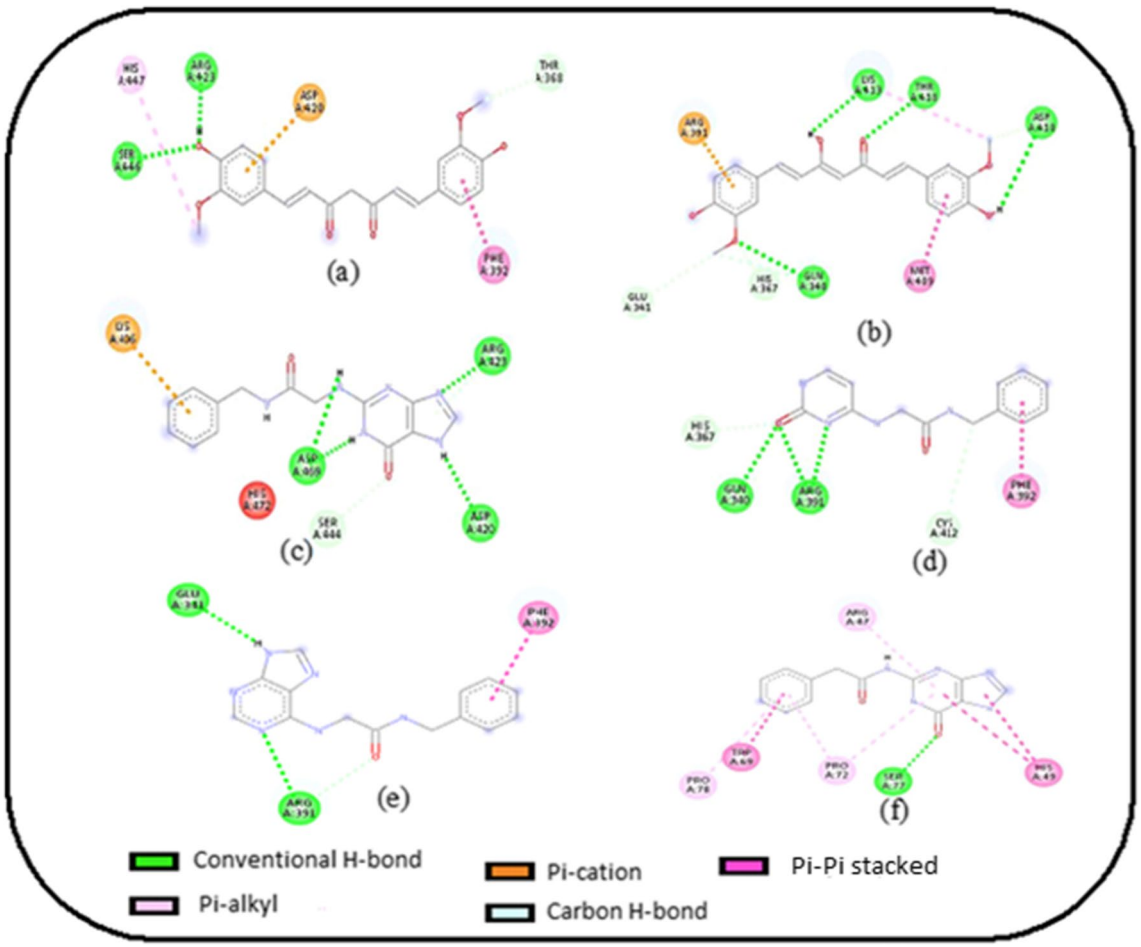

Fig. 2 Interactions between 5ZLN site with **a** Compound 1**b** Compound 2 **c** Compound 3 **d** Compound 4 **e** Compound 5 **f** Compound 9

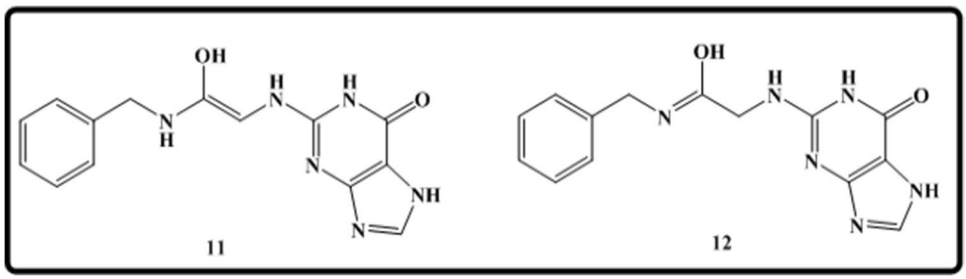

Fig. 3 Tautomeric forms of compound 3 enolic form (11) iminium form (12)

through TLR9 for the treatment of cancer are still under trial [6, 37]. Presently, docking analysis against breast cancer target site (4RJ3) was carried out and compared with curcumin (Table 2) [38]. Compounds 2 and 3 have shown high efficiency in their binding energies when compared with curcumin. Further, it was seen that the enolic form (2) has shown increased potency in terms of binding energy for various target sites than keto form (1). Finer details of structural features between keto and enol forms of curcumin made us extend our studies for different tautomeric forms of compound 3 as shown in Fig. 3.

Table 3 Binding energies of compounds 11 and 12 toward 4RJ3, 4YOJ, 4YO9, and 1I1R (kcal/mol)

Compound	4RJ3	4YOJ	4YO9	1I1R
11	**– 8.5**	**– 7.5**	**– 7.6**	**– 7.2**
12	– 7.4	– 7.2	– 7.1	– 7.0

The significance of bold values is for the more efficient results

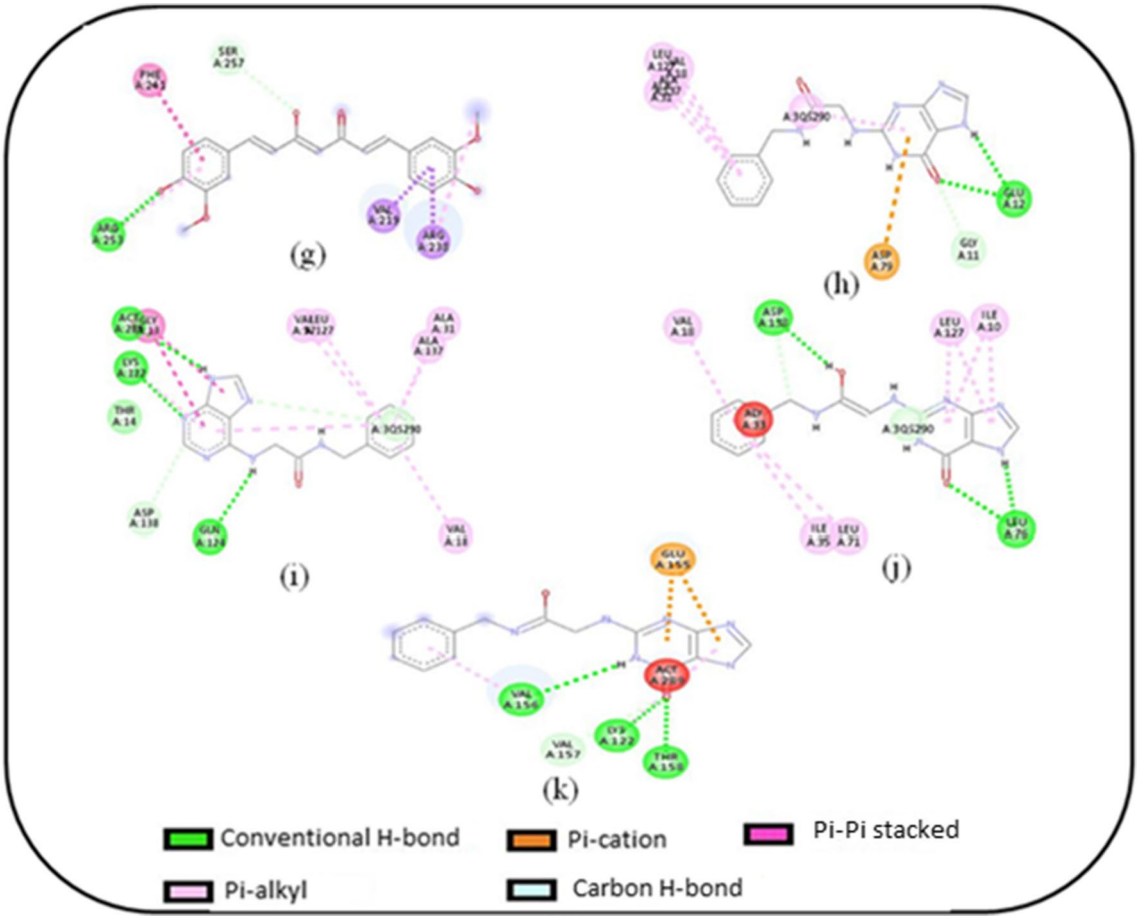

Fig. 4 Interactions between 4RJ3 site with **g** Compound 2 h Compound 3 **i** Compound 5 **j** Compound 11 k Compound 12

Out of these 3 different forms of compound 3, the enolic form (11) has shown most efficient results in terms of binding energy toward 4RJ3 − 8.5 kcal/mol (Fig. 3 and Table 3). It may be due to the CHB interaction of hydroxyl group in the linker, similar to the enolic form of curcumin (2) (Fig. 4).

While comparing the structural interactions of tautomeric forms i.e., compound 3, 11, and 12, it was found that compound 12 interacted via CHB interaction with LYS 122 has a minimum bond distance of ~ 1.921 Å (ST-5). Further, minimum hydrophobic interactions were observed in the case of compound 12 as compared to the large number of these interactions of enolic (11) and keto form (3). Although, compound 12 has increased binding energy, but due to the minimum hydrophobic interactions, 12 may have better results. *Moreover, such studies have explored the new point for discussion that outer environmental parameters i.e., solvent potency which affects the flipping of H from one form to another might be involved in the interaction studies.*

Molecular docking studies of MERS-CoV (PDB ID: 4YOJ and 4YO9) with various ligands (1–5, 9–12)

Both SARS-CoV and MERS-CoV are emerging zoonotic pathogens that crossed the barriers to contaminate the human body [39]. Viral adaptations to human cells may have contributed to the increased replication, transmission, and pathogens of MERS-CoV in humans On the other hand, TLRs play an important role in reorganization of viral particles and the activation of the innate immune system [8]. Unfortunately, the exact pathway for understanding the pathogenesis of SARS-CoV and MERS-CoV is still under consideration.

Bat corona virus HKU4-3CL^{pro} bound to non-covalent inhibitor viral sites (PDB Code:—4YO9, 4YOG, 4YOI, 4YOJ) were targeted by keto and enol form of curcumin as shown in Table (ST-6). Curcumin has shown the most efficient binding results against two receptor sites i.e., 4YO9 and 4YOJ. Therefore, all other compounds were docked against both these target sites as shown in Table 2. Interestingly, compound 3 has shown minimum binding energy among all other compounds. Broadly, it has been observed

that hydrogen bond interactions and hydrophobic interaction greatly influenced the binding energies. Introduction of hetero atom in the linker part as well as in the aromatic system was found to be important for the binding efficacy of a particular ligand.

Molecular docking studies of cytokine site (PDB ID: 1I1R) with various ligands (1–5, 9–12)

Cytokines are responsible for regulating the immune system and generate T cells and B cells which resulted in pro-inflammation. Out of various interleukin cells, IL-6 has been widely expanded due to its upregulation during acute viral infection. Further, IL-6 invention has been associated with both pro and anti-inflammatory actions [40]. *After critically investigating the binding energies of the compounds (1–5 and 9–12), using 1I1R as receptor site for IL-6, it has been examined that here also, compound 3 has resulted with greater efficiency in terms of binding energies as well as structural interactions* (Tables 2 and 3).

Structural features of compound 3 toward various target sites as a multi-targeted action

As discussed previously, the efficiency of compound 3 toward 5ZLN, 4RJ3, 4YOJ, 4YO9, and 1I1R was due to its lowest binding energies (Table 2). Further, structural interactions of compound 3 toward these sites have clearly shown that the presence of nitrogen in the linker is responsible for good binding interaction with minimum bond distance (Table 4).

Moreover, Compound 3 exhibited only two conventional hydrogen bond interactions toward 4RJ3, whereas it showed three hydrogen bond interactions toward 1I1R, five and four for 4YO9 and 4YOJ, respectively. *Although a greater number of interactions may not be the only factor in binding toward the receptors, but the orientation of a ligand in the binding pocket of these sites played crucial role for better interactions.* Both binding energies and structural interactions of compound 3 proved it to be a multifaceted compound with increased potency toward interleukin-6 (IL-6), 4YOJ, and 4YO9 sites. The molecular dynamics simulation of compound 3 is further selected to study and analyze its stability toward 5ZLN, 4RJ3, 4YO9, and 1I1R target sites (Fig. 5).

Table 4 Linker interactions toward various target sites of compound 3

Proteins	Amino acids	Bond distance	Interactions	Bond type
5ZLN	ASP A: 469	2.0217	N-2a	CHB
4RJ3	–	–	–	–
4YOJ	PRO A:111	1.80284	N-2a	CHB
4YO9	CYS A: 148	2.32599	O of C-1	CHB
	SER A: 147	2.5998	O of C-1	
	GLY A: 146	2.3259	O of C-1	
	GLN A: 167	2.92729	N-1a	
1I1R	GLU A: 129	2.50783	N-2a	CHB

Molecular dynamics simulation

Molecular dynamics simulations were performed on the top hits containing high binding energies. Over the simulation period, the projected conformational changes from the initial structure were presented in terms of root mean square deviation (RMSD). Moreover, structural stability, atomic mobility, and residue flexibility at times of interaction of protein-hit were expressed with root mean square fluctuation (RMSF) values [41, 42]. The peaks of the RMSF graph represent the fluctuation portion of the protein through the simulation. The *N*- and *C*-terminal have shown more changes than any other portion of the protein. Alpha helices and beta strands showed less fluctuation, as they were stiffer than the unstructured part of protein, as well as the loop portion. The RMSD showed a small deviation initially till 40 ns and then there was a small flip and the system gets equilibrated throughout the simulation. The complex was stable throughout the simulation, ligand remained inside the binding pocket and made important interactions and the backbone was consistent. The deviation might be due to conformational changes as shown in Fig. 6. Similarly, estimated RMSF values less than 3 Å indicated high stability of the complex and there was very small fluctuation where ligand made interaction with the receptor as shown in Fig. 7. The RMSD of 4RJ3 complex showed variation initially till 50 ns and then simulation was equilibrated and there was not much abnormal deviation observed throughout 100 ns. The deviation may be due to flexibility of the ligand. For RMSF, there was fluctuation for LUE 37, PRO 38, and SER 39, and the remaining structure was more stable comparatively, and there was not much fluctuation where ligand made contacts with protein. The complex of 4YO9 showed a very small deviation till 50 ns and then it was consistent and conserved over the MD simulation. The variation of RMSF was observed with small fluctuation for only ILE 72, GLY 73, and ALA 74. There was no abnormal fluctuation where the ligand made contact. The complex of 5ZLN showed deviation till almost 60 ns after that simulation was equilibrated. The fluctuation in the RMSF graph was a little high for SER 404, THR 405, and LYS 406. There was a very small fluctuation where ligands made contacts.

The complex of 1I1R has shown significantly different types of intermolecular interactions during the entire simulation including hydrogen bonds, ionic, water bridges,

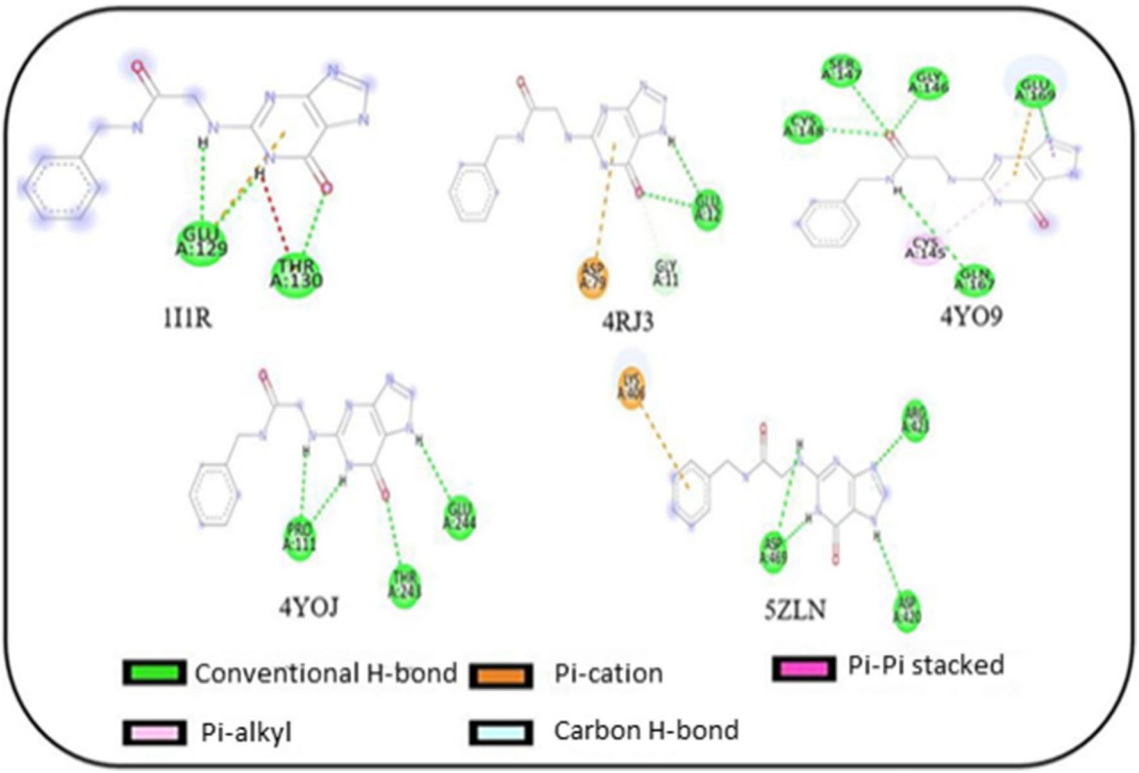

Fig. 5 2D Interactions of compound 3 toward different target sites

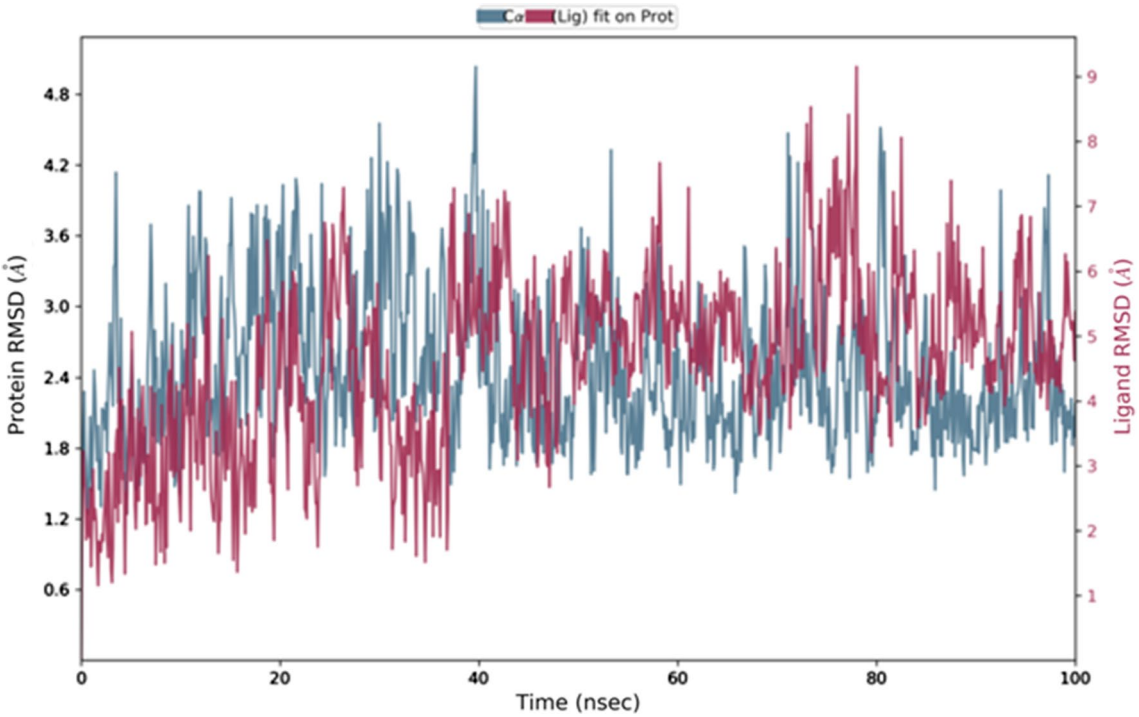

Fig. 6 Root mean square deviation plot of 1I1R Complex

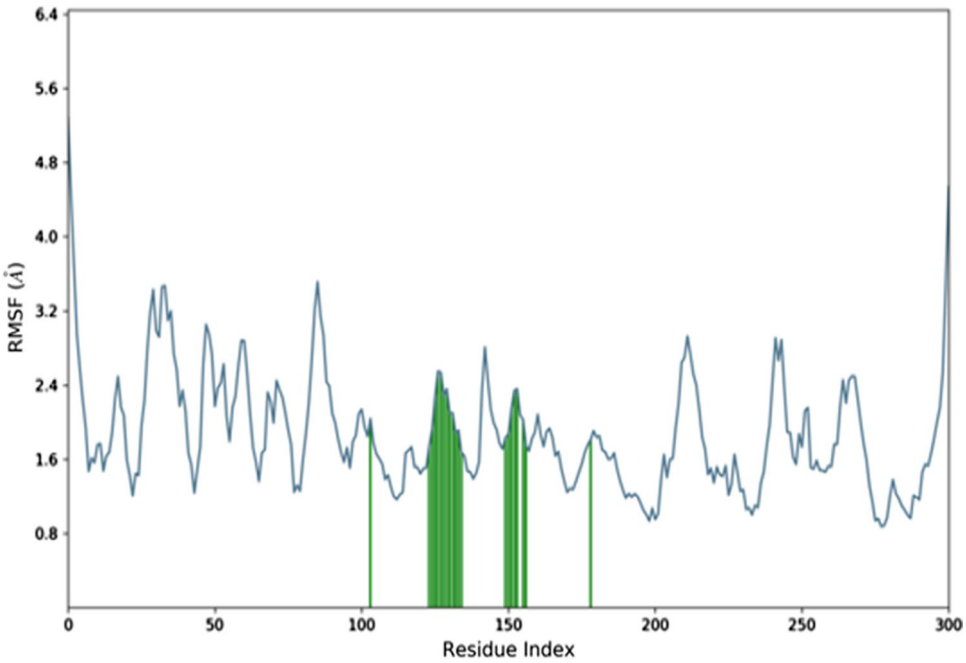

Fig. 7 Root mean square fluctuation plot of 1I1R Complex

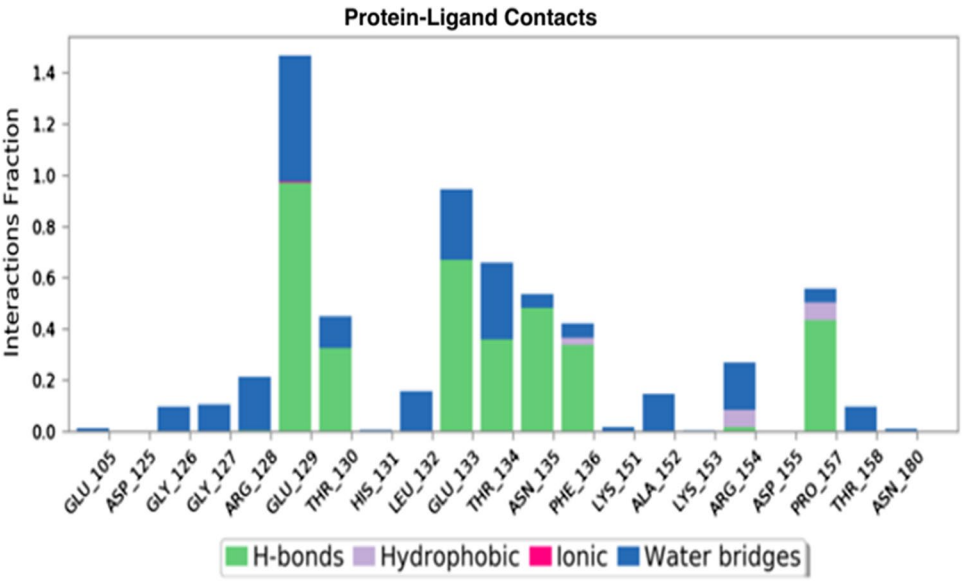

Fig. 8 Protein–ligand contacts of 1I1R Complex

and hydrophobic. The residues participating in these interactions include GLUY 105, ASP 125, GLY 126, GLY 127, ARG 128, GLU 129, THR 130, HIS 131, GLU 133, ASN 135, THR 134, PHE 136, LYS 151, ALA 152, LYS 153, ARG 154, ASP 155, PRO 157, and THR 158 as shown in Fig. 8. Complex of 4RJ3 showed interactions with LYS 9, GLY 11, GLY 13, VAL 18, ALY 33, VAL 57, PHE 75, LEU 76, HIS 77, LYS 81, ASP 120, LYS 122, ASN 125, and ALA 137. Similarly, the interacting residues of complex of 4YO9 include MET 25, LEU 27, HIS 41 ALA 46, CYS 145, GLY 146, SER 147, CYS 148, GLN 167, MET 168, GLU 169, GLU 189, ASP 190, LYS 191, THR 193, HIS 194, and GLN 195.

The complex of 5ZLN also showed interactions with LYS 406, ASN 407, PHE 408, ARG 411, ARG 423, SER 446, HIS 447, VAL 467, ASP 469, SER 471, ALA 491, LEU 492, ASP 493, SER 495, TYR 496, SER 521, LEU 522, SER 523, ALA 525, PHE 544, ASP 546, LYS 574, and SER 578.

The 1I1R complex was studied to find out the influence of the ligand on over all proteins. Six properties were examined to illustrate the stabilities of the selected ligands in the binding pocket during the simulation of 100 ns as shown in (a), (b), and (c): (1) Ligand RMSD:

Root mean square deviation of a ligand with respect to the reference conformation (typically the first frame was used as the reference and it was regarded as time $t = 0$); (2) Radius of gyration (rGyr): It was used to measure the 'extendedness' of a ligand, and was equivalent to its principal moment of inertia; (3) intramolecular hydrogen bond (intraHB): Number of internal hydrogen bonds (HB) within a ligand molecule. (4) Molecular surface area (MolSA): Molecular surface was calculated with a value of 1.4 Å probe radius; (5) Solvent accessible surface area (SASA): Molecular surface area of accessible by a water molecule; (6) Polar surface area (PSA): Solvent accessible surface area in a molecule contributed only by oxygen and nitrogen atoms.

As shown in Fig. 9, the RMSD of the ligand was nearly 1.5 Å from almost 0 ns to 45 ns and it was almost 2.8 Å till 100 ns. The rGyr value of ligand in the binding pocket can be divided into two stages, the values were 3–4 Å from 0 ns to almost 45 ns and then it was stable at 4–4.5 Å after 45 ns till the end of simulation and the constant values indicated the steady behavior. The intraHB, MolSA, SASA, and PSA plots also indicated the consistency of the ligand during the whole simulation process. In the MolSA, SASA, and PSA plots for the ligand, there was small fluctuation till almost 40 ns consistently and curves were smooth after 40 ns. These curves discovered the consistency of the ligands in the binding pocket over the simulation trajectory.

Further, compound 3 was subjected for in vitro anti-inflammatory activity based on docking analysis and molecular dynamics simulation because it has shown good binding results.

Biological activity

Membrane stability method

A variety of disorders was found as a result of inflammation caused by lysosomal enzymes. They are well known for their extracellular activity such as acute inflammation. (NSAIDS) are best known for their anti-inflammatory activity. They act either by the inhibition of lysosomal enzymes or by stabilizing the lysosomal membrane. It is well known that HRBC membrane is similar to the lysosomal membrane. Therefore, this method was used to check the stability of HRBC membrane to predict the anti-inflammatory activity of the new compound in comparison to the reference molecule [43]. Thus, compound 3 along with reference molecule was incubated at 100 µg/ml for 30 min at 37 °C with HRBC solution. The percentage of hemolysis and percentage of protection was calculated.

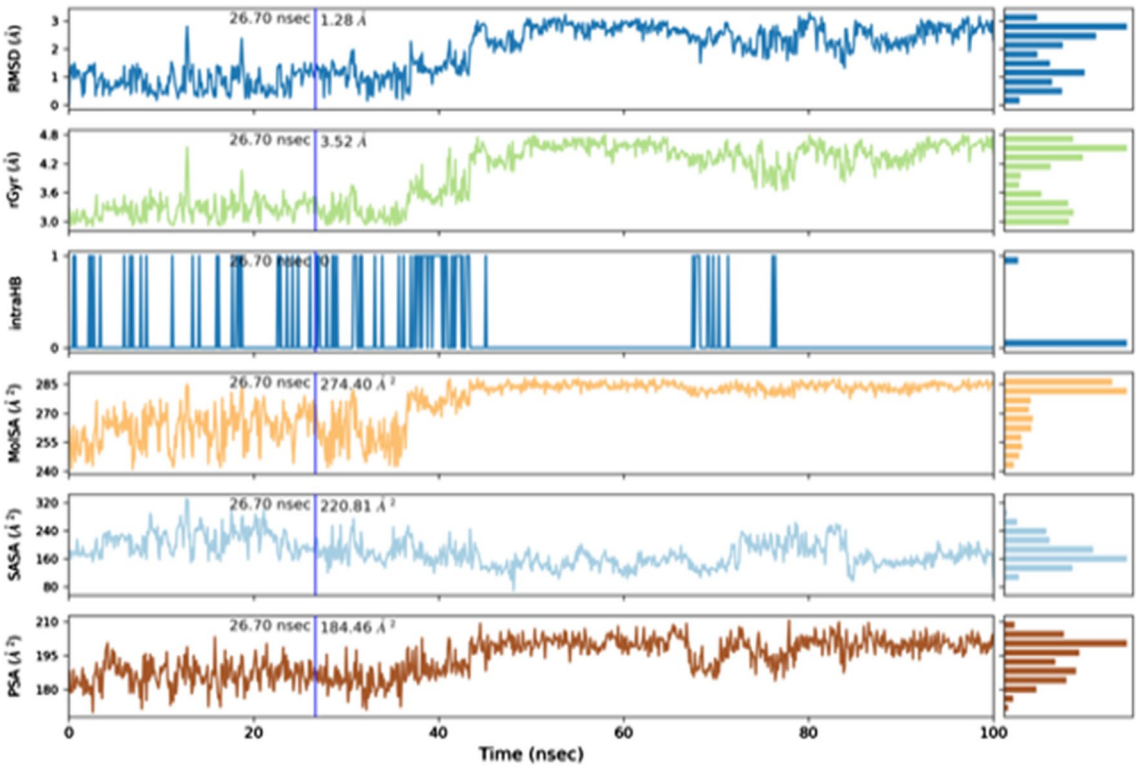

Fig. 9 Variation in the ligand's properties w.r.t time during the course of 100 ns simulation

Table 5 Percentage (%) of hemolysis and protection

Compound	Hemolysis (%)	Protection (%)
Control	0.0	0.0
1	45.4	42.43
3	57.5	54.55
Diclofenac	59.1	40.9

Anti-inflammatory activity in vitro

Compound 3 was screened for anti-inflammatory activity using Membrane Stability Method [43]. The result of compound 3 has been compared with curcumin and diclofenac. It has shown significant results as compared to curcumin in hemolysis as shown in Table 5.

Conclusion

Multifaceted actions of compound 3 have shown remarkable results against TLR9 sites, breast cancer (4RJ3), viral proteins (4YO9 and 4YOJ) sites, and most important interleukin-6 (1I1R) site. The protein–ligand interactions of compound 3 toward all these sites in comparison to curcumin and some similar compounds have depicted its efficient results not only in terms of binding energy but in their structural interactions also. Moreover, out of three tautomeric forms of compound 3 i.e., 3, 11, and 12, it was seen that the presence of enolic form was important for the better interactions as compared to its keto form. More refined results were obtained after analyzing the stabilization of compound 3 toward all their sites at 100 ns in molecular dynamics simulation. Compound 3 has shown excellent stabilization results for 1I1R site. In vitro studies for anti-inflammatory activity further extended the results and exhibited the efficacy of compound 3 in all fields.

Methods

Material

A-chloroacetyl chloride, Guanine, adenine, and cytosine were purchased from Avra synthesis. The melting points were recorded by the open capillary method. Sodium chloride, methanol, acetonitrile, and dichloromethane were of Lobachem. The IR spectra were obtained by Perkin Elmer RXIFT Infrared spectrophotometer. NMR spectra were recorded on Bruker Avance 500 MHz spectrophotometer with TMS as an internal standard. The mass spectra were recorded on the Waters Micromass Q-T of Micro (HRMS) spectrometer.

Experiment

Synthesis of N-benzyl-2-chloroacetamide (3′)

9 mmol (0.963 g) of benzylamine and 9 mmol of trimethylamine were stirred with 40 ml dichloromethane (DCM) for 36–37 h with temperature variation of 0 °C-5 °C initially for 1 h followed by 1.1 ml (14 mmol) of *a*-chloroacetyl chloride. The formation of the product was monitored by thin-layer chromatography using methanol and chloroform (1:4) as mobile phase. The reaction mixture was filtered, and the resulting solid was dissolved in dichloromethane. The organic layer was dried over anhydrous sodium sulfate, and after the removal of solvent, pure sample was obtained (Scheme 1) [44, 45].

Coupling reaction of N-benzyl-2-chloroacetamide (3′) with various DNA bases to synthesize 3, 4, and 5

35 ml of acetonitrile (ACN) was added to 1.2 mmol of *N*-benzyl-2-chloroacetamide. The reaction mixture was stirred for 49–50 h after the addition of 2.4 mmol triethylamine, 1.2 mmol of sodium iodide, and 2.4 mmol of DNA bases. The formation of the product was examined by thin-layer chromatography by methanol and chloroform (1:4). The reaction was filtered and resulting solid was dissolved in acetonitrile. The compound was extracted using petroleum ether, further pure compound was collected after recrystallization using acetonitrile [45–49].

Physical properties and spectroscopic data

N-benzyl-2-chloroacetamide (3′)

Brown, yield = 60.9%, mp = 148 °C–150 °C. **IR cm^{-1}**: ν_{max} 3279.27 (N–H str.); 3063.55, 3030.51 (Ar C–H str.); 2881.88 (Aliphatic C-H str.); **^{1}H-NMR** (400 MHz, $CDCl_3$) δ (ppm): 7.32 (m, 3H), 7.22 (m, 2H), 6.84 (s, 1H), 4.42 (d, 2H), 4.02 (s, 2H).

N-benzyl-2-((6-oxo-6,7-dihydro-1H-purine-2-yl)amino) acetamide (3)

Cream, yield = 64.5%, mp = 300 °C–302 °C**. IR cm^{-1}**: ν_{max} 3276.55 (N–H str.); 3061.95 (Ar C–H str.); 2917.76, 2849.51 (Aliphatic C–H str.), 1640.29 (C = O; amide), 1604.40 (C = O; amide); **^{1}H-NMR** (400 MHz, $CDCl_3$) δ (ppm): 7.37 (dd, J = 15.2 Hz, 3H), 7.31 (dd, J = 14.4 Hz, 4H), 6.88 (brs, NH, D_2O exchangeable), 6.31 (brs, NH, D_2O exchangeable), 4.56 (dd, 2H), 4.13 (s, 1H), 3.74 (s, 1H), 1.66 (s, 1H, D_2O exchangeable); **^{13}C-NMR** (125 MHz, $CDCl_3$) δ (ppm): 167.68, 166.71, 166.03, 139.76, 137.40, 130.11, 129.48,

Scheme 1 Synthesis of new compounds

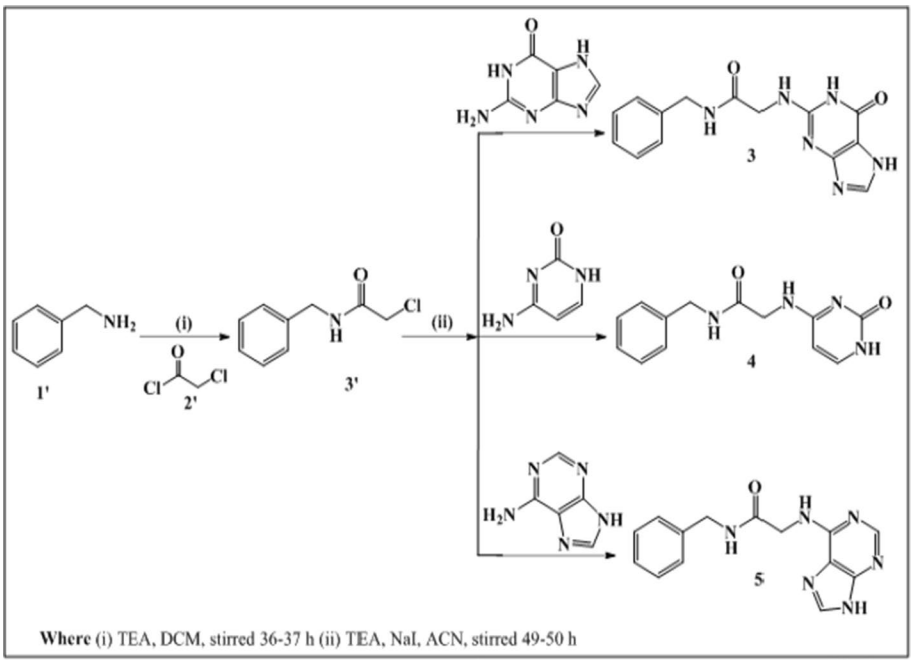

128.49, 127.82, 45.05, 30.26; **HR-MS:** Molecular ion peak (M + 3) = 301, base peak = 275, daughter ion peaks = 274, 212, 198, 150.

N-benzyl-2-((2-oxo-1,2-dihydropyrimidine-5-yl)amino) acetamide (4)

Yellow, yield = 67.2%, mp = 278 °C–280 °C**. IR cm**$^{-1}$ 3288.12 (N–H str.), 3062.53 (Ar C–H str.), 2924.90 (Aliphatic C–H str.), 1651.41 (C = O str), 1241.82 (C–N str.); **^{1}H-NMR** (500 MHz, $CDCl_3$) δ (ppm): 7.73 (brs, 1H), 7.36 (dd, J = 9.4 Hz, 4H), 7.30 (dd, J = 7.5, 3H), 6.38 (brs, 1H), 4.51 (dd, 2H), 4.18 (s, 1H), 3.73 (s, 1H), 1.68 (s, 1H); **^{13}C-NMR** (125 MHz, $CDCl_3$) δ (ppm): 167.50, 166.66, 162.78, 138.18, 137.34, 136.97, 130.47, 129.99, 128.65, 127.86, 127.42, 126.56, 55.57, 44.81; **HR-MS:** Molecular ion peak (M + H_2O) = 276, base peak = 249, daughter ion peaks = 197, 91.

2-((9H-purin-6-yl)amino)-N-benzylacetamide (5)

Light Yellow, yield = 69.3%, mp = 270 °C–272 °C**. IR cm**$^{-1}$ 3277.34 (N–H str.), 3060.69 (Ar C–H str.), 2923.36 (Aliphatic C–H str.), 1639.41 (C = O str), 1237.70 (C–N str.); **^{1}H-NMR** (500 MHz, $CDCl_3$) δ (ppm): 7.35 (m, 3H), 7.29 (m, J = 9.4 Hz, 4H), 6.87 (brs, 1H), 6.35 (s, 1H), 4.50 (d, 1H), 4.46 (s, 1H), 4.10 (s, 1H), 2.05 (s, 1H); **^{13}C-NMR** (125 MHz, $CDCl_3$) δ (ppm): 167.68, 166.85, 140.10, 137.96, 130.62, 129.80, 128.88, 128.48, 128.04, 125.07, 115.14, 45.36, 30.34; **HRMS:** Molecular ion peak = (M + 1) = 283, base peak = 298.

Supplementary Information The online version contains supplementary material available at https://doi.org/10.1007/s11030-023-10616-8.

Acknowledgements Two of the authors, Mandeep Kaur and Amandeep Kaur, are grateful to CSIR New Delhi, India, for providing financial support for carrying out the Ph. D. work. We are highly thankful to RSIC, Panjab University, Chandigarh and IIT Ropar for spectroscopic analysis and Sophisticated Instrument Centre, Punjabi University, Patiala. Also, we are highly thankful to Dr. Siddalingeshwar K G (Quality Manager, Head, R & D) Scientific & Industrial Research Centre, Bangalore for their biological activities.

References

1. Akira S, Uematsu S, Takeuchi O (2006) Pathogen recognition and innate immunity. Cell 124:783–801. https://doi.org/10.1016/j.cell.2006.02.015
2. Hagerling C, Casbon AJ, Werb Z (2015) Balancing the innate immune system in tumor development. Trends Cell Biol 25:214–220. https://doi.org/10.1016/j.tcb.2014.11.001
3. Sun L, Jiang Q, Zhang Y, Liang H, Ren H, Zhang D (2016) Toll-like receptors and breast cancer. Integer Cancer Sci Therap 3:432–436. https://doi.org/10.15761/ICST.1000183
4. Yusuf N (2014) Toll-like receptor mediated regulation of breast cancer: a case of mixed blessings. Front Immunol 5:224. https://doi.org/10.3389/fimmu.2014.00224
5. Bhattacharya D, Yusuf N (2012) Expression of Toll-like receptors on breast tumors: taking toll on tumor microenvironment. Int J Breast cancer 2012:1–7. https://doi.org/10.1155/2012/716564
6. Sandholm J, Salander KS (2014) Toll-like receptor 9 in breast cancer. Front Immunol 5:330. https://doi.org/10.3389/fimmu.2014.00330

7. Krieg AM (2008) Toll-like receptor 9 (TLR9) agonists in the treatment of cancer. Oncogene 27:161–167. https://doi.org/10.1038/sj.onc.1210911
8. Khanmohammadi S, Rezaei N (2021) Role of toll-like receptors in the pathogenesis of COVID-19. J Med Virol 93:2735–2739. https://doi.org/10.1002/jmv.26826
9. Bezemer GFG, Garssen J (2021) TLR9 and COVID-19: A multidisciplinary theory of a multifaceted therapeutic target. Front Pharmacol. https://doi.org/10.3389/fphar.2020.601685
10. Lester SN, Li K (2014) Toll-like receptors in antiviral innate immunity. J Mol Biol 426:1246–1264. https://doi.org/10.1016/j.jmb.2013.11.024
11. Carty M, Bowie AG (2010) Recent insights into the role of toll-like receptors in viral infections. Clin Exp Immunol 161:397–406. https://doi.org/10.1111/j.1365-2249.2010.04196.x
12. Mojtabavi H, Saghazadeh A, Rezaei N (2020) Interleukin-6 and severe COVID-19: a systematic review and meta-analysis. Eur Cytokine Netw 31:44–49. https://doi.org/10.1684/ecn.2020.0448
13. Lotfi M, Rezaei N (2020) SARS-CoV-2: a comprehensive review from pathogenicity of the virus to clinical consequences. J Med Virol 92:1864–1874. https://doi.org/10.1002/jmv.26123
14. Alnefaie A, Albogami S (2020) Current approaches used in treating COVID-19 from a molecular mechanisms and immune response perspective. Saudi Pharm J 28:1333–1352. https://doi.org/10.1016/j.jsps.2020.08.024
15. Saghazadeh A, Rezaei N (2017) Implications of toll-like receptors in Ebola infection. Expert Opin Ther Targets 21:415–425. https://doi.org/10.1080/14728222.2017.1299128
16. Babaei F, Nassiri-Asi M, Hosseinzadeh H (2020) Curcumin (a constituent of turmeric): new treatment option against COVID-19. Food Sci Nutr 8:5215–5227. https://doi.org/10.1002/fsn3.1858
17. Mbese Z, Khwaza V, Aderibigbe BA (2019) Curcumin and its derivatives as potential therapeutic agents in prostate, colon and breast cancers. Molecules 24:4386. https://doi.org/10.3390/molecules24234386
18. Lee DY, Hou YC, Yang JS, Lin HY, Chang TY, Lee KH, Kuo SC, Hsieh MT (2020) Synthesis, anticancer activity, and preliminary pharmacokinetic evaluation of 4,4-disubstituted curcuminoid 2,2-is(hydroxymethyl)propionate derivatives. Molecules 25:479. https://doi.org/10.3390/molecules25030479
19. Prasetyaningrum PW, Bahtiar A, Hayun H (2018) Synthesis and cytotoxicity evaluation of novel asymmetrical mono-carbonyl analogs of curcumin (AMACs) against Vero, HeLa, and MCF7 cell lines. Sci Pharm 86:25. https://doi.org/10.3390/scipharm86020025
20. Shabaninejad Z, Pourhanifeh MH, Movahedpour A, Mottaghi R, Nickdasti A, Mortezapour E, Shafiee A, Hajighadimi S, Moradizarmehri S, Sadeghian M, Mousavi SM, Mirzaei H (2020) Therapeutic potentials of curcumin in the treatment of Glioblstoma. Eur J Med Chem. https://doi.org/10.1016/j.ejmech.2020.112040
21. Kim BR, Park JY, Jeong HJ, Kwon HJ, Park SJ, Lee IC, Ryu YB, Lee WS (2018) Design, synthesis, and evaluation of curcumin analogues as potential inhibitors of bacterial sialidase. J Enzyme Inhib Med Chem 33:1256–1265. https://doi.org/10.1080/14756366.2018.1488695
22. Amalraj A, Pius A, Gopi S, Gopi S (2017) Biological activities of curcuminoids, other biomolecules from turmeric and their derivatives-a review. J Tradit Complement Med 7:205–233. https://doi.org/10.1016/j.jtcme.2016.05.005
23. Kaur G, Kaur M, Bansal M (2021) Review article new insights of structural activity relationship of curcumin and correlating their efficacy in anticancer studies with some other similar molecules. Am J Cancer Res 11:3755–3765
24. Patel A, Rajendran M, Shah A, Patel H, Pakala SB, Karyala P (2020) Virtual screening of curcumin and its analogs against the spike surface glycoprotein of SARS-CoV-2 and SARS-CoV. J Biomol 40:5138–5146. https://doi.org/10.1080/07391102.2020.1868338
25. Yadav B, Taurin S, Rosengren RJ, Schumacher M, Diederich M, Somers-Edgars TJ, Larsen L (2010) Synthesis and cytotoxic potential of heterocyclic cyclohexanone analogues of curcumin. Bioorg Med Chem 18:6701–6707. https://doi.org/10.1016/j.bmc.2010.07.063
26. Bhawana BRK, Buttar HS, Jain VK, Jain N (2011) Curcumin Nanoparticles: preparation, characterization, and antimicrobial study. J Agric Food Chem 59:2056–2061. https://doi.org/10.1021/jf104402t
27. Tomeh MA, Hadianamrei R, Zhao X (2019) A review of curcumin and its derivatives as anticancer agents. Int J Mol Sci 20:1033. https://doi.org/10.3390/ijms20051033
28. Bonaccorsi PM, Labbozzetta M, Barattucci A, Salerno TMG, Poma P, Notarbartolo M (2019) Synthesis of curcumin derivatives and analysis of their antitumor effects in triple negative breast cancer (TNBC) cell lines. Pharmaceuticals 12:161. https://doi.org/10.3390/ph12040161
29. Wang R, Zhang X, Chen C, Chen G, Zhong Q, Zhang Q, Zheng S, Wang G, Chen QH (2016) Synthesis and evaluation of 1,7-diheteroarylhepta-1,4,6-trien-3-ones as curcumin-based anticancer agents. Eur J Med Chem 110:164–180. https://doi.org/10.1016/j.ejmech.2016.01.017
30. Veber DF, Johnson SR, Cheng HY, Smith BR, Ward KW, Kopple KD (2002) Molecular properties that influence the oral bioavailability of drug candidates. J Med Chem 45:2615–2623. https://doi.org/10.1021/jm020017n
31. Pajouhesh H, Lenz GR (2005) Medicinal chemical properties of successful central nervous system drugs. NeuroRx 2:541–553. https://doi.org/10.1602/neurorx.2.4.541
32. Zhang YY, Liu H, Summerfield SG, Luscombe CN, Sahi J (2016) Integrating *in silico* and *in vitro* approaches to predict drug accessibility to the central nervous system. Mol Pharmaceutics 13:1540–1550. https://doi.org/10.1021/acs.molpharmaceut.6b00031
33. Rankovic Z (2015) CNS drug design: balancing physicochemical properties for optimal brain exposure. J Med Chem 58:2584–2608. https://doi.org/10.1021/jm501535r
34. Abdel-Aziz AA, El-Azab AS, Alanazi AM, Asiri YA, Al-Suwaidan IA, Maarouf AR, Ayyad RR, Shawer TZ (2016) Synthesis and potential antitumor activity of 7-(4-substituted piperazin-1-yl)-4-oxoquinolines based on ciprofloxacin and norfloxacin scaffolds: *in silico* studies. J Enzyme Inhib Med Chem 31:796–809. https://doi.org/10.3109/14756366.2015.1069288
35. Shimizu M, Wada T, Oka N, Saigo K (2004) A novel method for the synthesis of dinucleoside boranophosphates by a boranophosphotriester method. J Org Chem 69:5261–5268. https://doi.org/10.1021/jo0493875
36. PubChem CID 115657068. https://pubchem.ncbi.nlm.nih.gov/compound/N-benzyl-2-_2-oxo-1H-pyrazin-3-yl_amino_acetamide. Accessed 29 Jan 2016
37. Kang TH, Mao CP, Kim YS, Kim TW, Yang A, Lam B, Tseng SH, Farmer E, Park YM, Hung CF (2019) TLR9 acts as a sensor for tumor-released DNA to modulate anti-tumor immunity after chemotherapy. J Immunother Cancer 7:1–8. https://doi.org/10.1186/s40425-019-0738-2
38. Rathinasabapathy P, Subramanian S, Duraisamy K (2017) Comparative *in silico* docking analysis of curcumin and resveratol on breast cancer proteins and their synergistic effect on MCF-7 cell line. J Young Pharm 9:480–485. https://doi.org/10.5530/JYP.2017.9.94
39. Hu B, Ge X, Wang LF, Shi Z (2015) Bat origin of human coroviruses. Virol J. https://doi.org/10.1186/s12985-015-0422-1

40. Velazquez-Salinas L, Verdugo-Rodriguez A, Rodriguez LL, Borca MV (2019) The role of interleukin 6 during viral infections. Front Microbiol 10:1057. https://doi.org/10.3389/fmicb.2019.01057
41. Bowers KJ, Chow E, Xu H, Dror RO, Eastwood MP, Gregersen BA, Klepeis JL, Kolossvary I, Moraes MA, Sacerdoti FD, Salmon J, Shan Y, Shaw DE (2006) Molecular dynamics-scalable algorithms for molecular dynamics simulation on commodity clusters. In Proceedings of the SC'06: Proceedings of the 2006 ACM/IEEE Conference Supercomputing, Tampa, FL, USA, 11–17 November, 43. doi: https://doi.org/10.1109/SC.2006.54
42. El Khatabi K, El-mernissi R, Moukhliss Y, Hajji H, Rehman HM, Yadav R, Lakhlifi T, Ajana MA, Bouachrine M (2022) Rational design of novel potential EGFR inhibitors by 3D-QSAR, molecular docking, molecular dynamics simulation, and pharmacokinetics studies. Chem Data Collect. https://doi.org/10.1016/j.cdc.2022.100851
43. James O, Nnacheta OP, Wara HS, Aliyu UR (2009) *In vitro* and *in vivo* studies membrane stabilization and cytotoxicity of water spinach from ipogi ponds (Nigeria). Int J PharmTech Res 1:474–482
44. Azema J, Guidetti B, Dewelle J, Le Calve B, Mijatovic T, Korolyov A, Vaysee J, Malet-Martino R, Kiss R (2009) 7-((4-Substituted)piperazin-1-yl) derivatives of ciprofloxacin synthesis and *in vitro* biological evaluation as potential antitumor agents. Bioorg Med Chem 17:5396–5407. https://doi.org/10.1016/j.bmc.2009.06.053
45. Kaur G, Kaur M, Sharad L, Bansal M (2019) Theoretical molecular predictions and antimicrobial activities of newly synthesized molecular hybrids of norfloxacin and ciprofloxacin. J Heterocyclic Chem 57:225–237. https://doi.org/10.1002/jhet.3768
46. Qandil M, Al-Zoubi LO, Al-Bakri AG, Amawi HA, Al-Balas QA, Alkatheriand AM, Albekairy AM (2014) Synthesis, antibacterial evaluation and QSAR of α-substituted-N_4- acetamides of ciprofloxacin and norfloxacin. Antibiotics 3:244–269. https://doi.org/10.3390/antibiotics3030244
47. Nami N, Tizkar M, Zardost MR (2017) Solvent-free synthesis of 2,6-dihydroxy-9H-purin and pteridine derivatives. J Heterocyclic Chem 54:3696–3699. https://doi.org/10.1002/jhet.2915
48. Milad HS, Asieh Y, Navabeh N (2012) Synthesis of novel 6-cyano-9-(aryl)-9H-purine derivatives via formamidine intermediates. E-J Chem 9:219–223. https://doi.org/10.1155/2012/762641
49. Nami Chemazi N, Nami N, Sheikh Bostanabad A (2022) Biosynthesis and characterization of Fe_3O_4/CaO nanoparticles and investigation of its catalytic property. J Nanostruct 12:160–169. https://doi.org/10.22052/JNS.2022.01.015

Authors and Affiliations

Gurmeet Kaur[1] · Manisha Bansal[3] · Hafiz Muzzammel Rehman[2] · Mandeep Kaur[1] · Amandeep Kaur[1]

[1] Synthetic and Medicinal Chemistry Laboratory, Department of Chemistry, Punjabi University, Patiala 147002, India

[2] School of Biochemistry and Biotechnology, University of the Punjab, Lahore, Punjab, Pakistan

[3] Department of Chemistry, Punjabi University, Patiala 147002, India